

DSS-13 26-Meter Antenna Upgraded Radiometer System

C. T. Stelzried
TDA Technology Development

L. Skjerve
Tracking Systems and Applications Section

G. Bury
TDA Mission Support and DSN Operations

The DSS-13 26-m antenna radiometer system has been upgraded with an IBM-compatible computer-controlled configuration with improved supporting hardware and software. Software has been generated to analyze results and correct for antenna mispointing, tropospheric loss, and other observing errors. This total power radiometer configuration provides a prototype for the new DSS-13 34-m antenna. The radiometer system is described in terms of the theory, instrumentation hardware, computer configuration, and operational features and performance. The system is used to obtain antenna efficiency and pointing model data and is useful for radio source calibrations required for radio astronomy. Some recent results are given.

I. Introduction

The highly productive DSS-13 26-m antenna radiometer system constructed by P. D. Batelaan et al. [1] more than 20 years ago became increasingly difficult to maintain due to a lack of replacement parts. This system has been replaced with an IBM-compatible computer-controlled configuration and improved supporting hardware and software. New calibration techniques provide increased measurement accuracy. This configuration is a prototype for the new DSS-13 34-m antenna radiometer system. The radiometer system improvements are described in terms of the theory, instrumentation hardware, computer configuration, and operational features and per-

formance. Noise temperature measurement errors in a microwave radiometer system due to receiver nonlinearities are small when a well-designed system is maintained and operated within the design range of amplifier signal levels. Nevertheless, it is necessary to quantify residual measurement errors and provide corrections when precision measurements are desired. Comparisons of the measured system noise temperature with different input signal levels obtained by switching between the antenna and ambient load are used to verify system linearity and to correct for system nonlinearity [2].

Radiometer development from 1987 to 1992 for the DSS-13 26-m antenna at both S-band (2.295 GHz) and

X-band (8.420 GHz)^{1,2,3,4} includes calibration methods and performance verification of the radiometer as used in the total power (TP) mode of operation using a single noise diode (ND). The radiometer system is useful for antenna efficiency and pointing offset measurements and radio source calibrations required for radio astronomy applications.

With proper receiver-amplifier signal levels and a power-meter detector, the linearity correction is very small. The power-meter output reading is highly linear with input power level, especially as compared with the square-law diode detectors designed in the 1970s. Using an ND at the receiver front end for determining system linearity is very useful for station equipment setup and performance monitoring. The measurements are all made from the control room for the operator's convenience. With good linearity, only verification but not correction for nonlinearity is necessary. This is usually not the case with presently available diode detectors, which, for accurate results, require correction for nonlinearity.

II. Total Power Radiometer System

Figure 1 is the DSS-13 26-m antenna block diagram for the antenna and control room; it shows the radiometer in the TP configuration. Simultaneous S- and X-band low-noise amplifiers are available with matching IF distribution amplifiers and power-meter detectors. The present two-channel radiometer system configuration is switchable for two S-band, two X-band, or one S-band and one X-band TP channels. The IBM PC system and microwave interface have been described previously.⁵ Radiometer calibration is obtained by switching the low-noise amplifier input into the microwave ambient termination and recording the power-meter levels with the ND on or off.

Figure 2 shows measurements of system noise temperature on the antenna (T_{op}) using the DSS-13 26-m antenna S-band system in the radiometer TP configuration. The

left side of Fig. 2 compares the uncorrected results of the diode detector with those of the power-meter. The right side compares the same data after corrections were applied for system nonlinearity. The agreement in T_{op} after correction is consistent with the nonlinear performance of the diode detector and the capability of the calibration technique to correct for nonlinearity. The power-meter detector is best used with strong and medium strength sources where accuracy is more important than minimum measurement resolution. The diode detector may be optimum for measurement resolution with some loss of accuracy associated with higher nonlinearity errors. Further performance testing will be required to compare the various combinations of S- and X-band amplifiers, TP and noise-adding radiometer (NAR) modes of operation, and power-meter and diode detectors. This comparison is needed to optimize the configuration for a particular measurement requirement. However, for most applications, the performance of the TP mode with a power-meter detector is satisfactory and justified by the configuration's simplicity.

The linearity correction factor for a power-meter configuration with proper amplifier level settings in the receiver system is typically less than 1 percent. For a well-designed system using the power-meter detector, the correction is unnecessary for most applications.

An example follows of the TP radiometer stability performance at the present stage of development. For December 14, 1989, data taken during radio source boresight observations, a measurement resolution of 0.006 K was obtained.⁶ The radiometer parameters for these observations were $T_{op} = 27.5$ K and B (bandwidth) = 19.2 Mhz, with a measurement time of 5 sec; these parameters resulted in a theoretical measurement resolution of 0.003 K. Therefore, such parameters as computer dead time, system gain instability, changing tropospheric effects, and radio-frequency interference reduce radiometer performance by about a factor of 2 for this example.

Future increased computer speed is expected to improve radiometer resolution performance by the reduction of dead time.

III. Radiometer Calibration Sequences

In addition to preobserving calibrations for the radiometer, shorter calibrations using the same data sequence as the precalibrations are performed during the

¹ C. T. Stelzried, *DSS-13 Radiometer System Status and Performance*, JPL D-9291 (internal document), Jet Propulsion Laboratory, Pasadena, California, January 1990.

² C. T. Stelzried, *Microwave Radiometers*, JPL D-9295 (internal document), Jet Propulsion Laboratory, Pasadena, California, August 1990.

³ L. J. Skjerve, *Preliminary Documentation for DSS-13 Radiometer Program*, JPL D-9292 (internal document), Jet Propulsion Laboratory, Pasadena, California, January 1990.

⁴ G. Bury, *DSS-13 Block Diagram*, JPL D-9300 (internal document), Jet Propulsion Laboratory, Pasadena, California, January 1990.

⁵ L. J. Skjerve, *DSS-13 26-m Antenna Radiometer Upgrade*, JPL D-9525 (internal document), Jet Propulsion Laboratory, Pasadena, California, March 1992.

⁶ Stelzried, *DSS-13 Radiometer System Status and Performance*, loc. cit.

observing session.⁷ These calibrations are called minicals and are used to correct for the amplifier gain changes associated with TP operation and in effect provide a slow Dicke-like switching radiometer mode of operation.

IV. Antenna Efficiency

Antenna efficiency in the DSN is defined with the atmosphere removed. The 5-point antenna boresight calibration data method⁸ is used to obtain radio source noise temperatures corrected for antenna mispointing.

The radio source noise temperatures for a 100-percent efficient antenna are evaluated from the source flux and angular size data.⁹ The ratio of measured to known radio source noise temperature defines antenna efficiency. As a function of elevation angle, EL, the antenna efficiency is represented by a second-order fit,

$$EFF = C0 + C1 \times EL + C2 \times EL^2 \quad (1)$$

For the DSS-13 26-m antenna, the 1991 results are given by

$$\left. \begin{array}{l} C0 = 0.56398, \\ C1 = 0.0003018, \\ C2 = -0.00000417 \end{array} \right\} \text{S-band}$$

$$\left. \begin{array}{l} C0 = 0.42120, \\ C1 = 0.0006582, \\ C2 = -0.00001867 \end{array} \right\} \text{X-band}$$

for 2.295 GHz (S-band) and 8.420 GHz (X-band), respectively. These represent maximum efficiencies of 0.569 at a 36.2-deg elevation angle and 0.427 at a 17.6-deg elevation angle for the S- and X-bands, respectively. Determination of these coefficients representing the change in efficiency with elevation angle is required to correct for the difference in elevation angle between the calibrators and unknown radio sources.

As discussed, it is necessary to correct for the radio source angular size relative to the antenna beamwidth. For

precise calibrations, a further complication arises if the antenna beamwidth is a function of the elevation angle, as shown in Fig. 3.

V. Radio Source Calibrations

Antenna efficiency measurements depend on assumed known radio source fluxes. The radiometer system is also used to measure unknown sources, usually relative to known sources.

An observing program is currently underway to monitor S- and X-band flux of the radio source 1830-211.¹⁰ Figure 4 shows a station observation log for 1991 DOY 352 data appropriate for 5-point on-off radio source data. The calibration data and observing sequence are computer controlled. This control includes antenna pointing, microwave switch control, and data collection. Data are alternately collected for the 1830-211 unknown source and calibrator known sources. A BASIC computer program compiled for use with IBM-compatible office computers and designated TPANxxxx (xxxx is currently version 0128)¹¹ is used to analyze the data. Figure 5 shows a printout of data file 06 for calibrator source 3C274 for DOY 352. Two data sequences, passes 1 and 2 for both X-band (IF1) and S-band (IF2), show the results of the analyzed observing data of the radio source temperature corrected for pointing offsets, atmospheric attenuation, antenna gain change with elevation, and source size.

The S- and X-band data are taken simultaneously with the radiometer system. The antenna pointing angular offsets for the 5-point data sequence are optimized for X-band, which has the narrowest beamwidth. The 5-point data sequence consists of an on-source measurement and off-source measurements with antenna angular offsets of ± 0.5 X-band beamwidths and ± 2.5 S-band beamwidths. The pointing offset is determined from the X-band data. The efficiency correction for the antenna pointing offset is applied directly for X-band and scaled by beamwidth for S-band. The S- and X-band beams are assumed to be coaligned.

Figure 6 shows the radiometer linearity and gain change as obtained from the minicals. The radiometer gain constants are updated after each minical, as the radiometer is presently operated. The gain correction is assumed to be

⁷ Ibid.

⁸ Ibid., Appendix C.

⁹ M. Klein and A. Freiley, *DSN Radio Source List for Antenna Calibration*, JPL D-3801, Rev. B (internal document), Jet Propulsion Laboratory, Pasadena, California, September 25, 1987.

¹⁰ M. Klein, personal communication, Space Physics and Astrophysics Section, Jet Propulsion Laboratory, Pasadena, California, November 1991.

¹¹ Skjerve, loc. cit.

the difference between the most recent minical and that computed from the curve fit at the time of the observation. Figure 7 shows a summary of the observations for X-band (IF1 = 12-MHz bandwidth). Some of the bad data are removed automatically by the computer (according to default criteria, such as pointing offsets, which result in greater than 15-percent correction to the source temperature) and further manually by the experimenter during postprocessing. For file 06, pass 1, X-band (IF1), the corrections modify the uncorrected on-off source temperature for 3C274 from 3.701 to 4.105 K. Figures 8 and 9 show the S- and X-band corrected fluxes measured during 1991 using this analysis. The standard deviations of the data relative to the straight-line fit are 0.28 and 0.20 flux units for the S- and X-bands, respectively.

Greater numbers of observed incidents of radio interference at S-band compared with those at X-band at DSS 13 are assumed to account for the higher S-band standard deviations. The high-electron mobility transfer (HEMT) amplifiers have gigahertz bandwidths with no filtering on their input. S- and X-band filtering at the input to the low-noise amplifiers will be provided in the future to reduce this effect.

Computer program TPAN0128 generates data files for all the raw and computed data. These files are further analyzed by the experimenter to provide the final scientific result.

VI. Conclusion

The TP radiometer mode of operation with the powermeter detector provides excellent measurement resolution and accuracy with a simple configuration. The TP mode utilizes modern stable amplifiers. Periodic radiometer calibrations during the observing period are used to remove long-term gain drifts. These minicals are used during post-data analysis for correcting the results. The NAR configuration is more complicated but should improve performance with amplifier gain changes.

The DSS-13 26-m antenna TP radiometer configuration continues to be upgraded. This system has been demonstrated during 1991 and continues operating in 1992 for engineering and science observations. Sample results obtained from the analysis program TPAN0128 are shown in Figs. 5, 7, 8, and 9.

Acknowledgments

Numerous people supported this activity and performed the measurements. DSS-13 personnel including J. Garnica, R. Rees, G. Farner, and R. Littlefair upgraded, modified, and documented the equipment and performed many hours of data taking and manipulation. C. Goodson and A. Price provided DSS-13 management support. M. Klein early on suggested collaboration between the radiometer development and data verification. This has been very beneficial to both activities and resulted in a universal radiometer system available for both station engineering activities, such as antenna boresighting and efficiency calibrations, and outside science application users.

References

- [1] P. D. Batelaan, R. M. Goldstein, and C. T. Stelzried, "A Noise Adding Radiometer for Use in the DSN," *Space Programs Summary 37-65*, vol. 2, Jet Propulsion Laboratory, Pasadena, California, pp. 66-69, September 30, 1970.
- [2] C. T. Stelzried, "Non-Linearity in Measurement Systems: Evaluation Method and Application to Microwave Radiometers," *TDA Progress Report 42-91*, vol. July-September 1987, Jet Propulsion Laboratory, Pasadena, California, pp. 57-66, November 15, 1987.

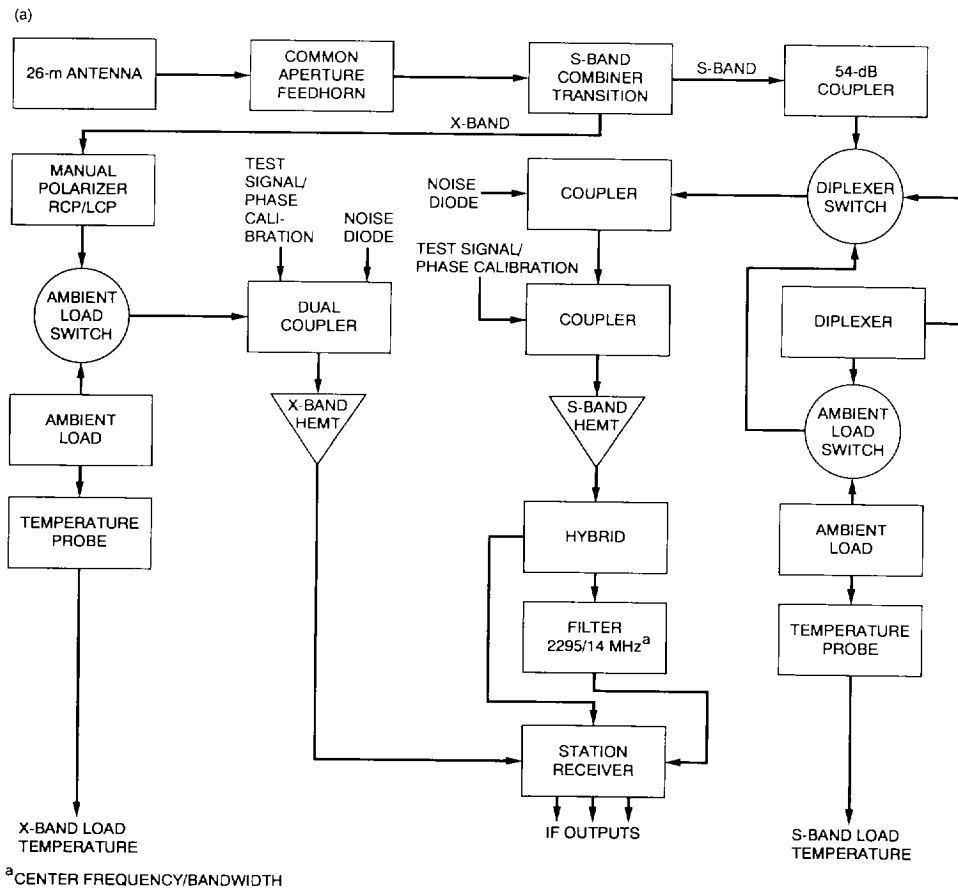


Fig. 1. DSS-13 26-m antenna system block diagram: (a) antenna feed cone assembly and (b) control room assembly.

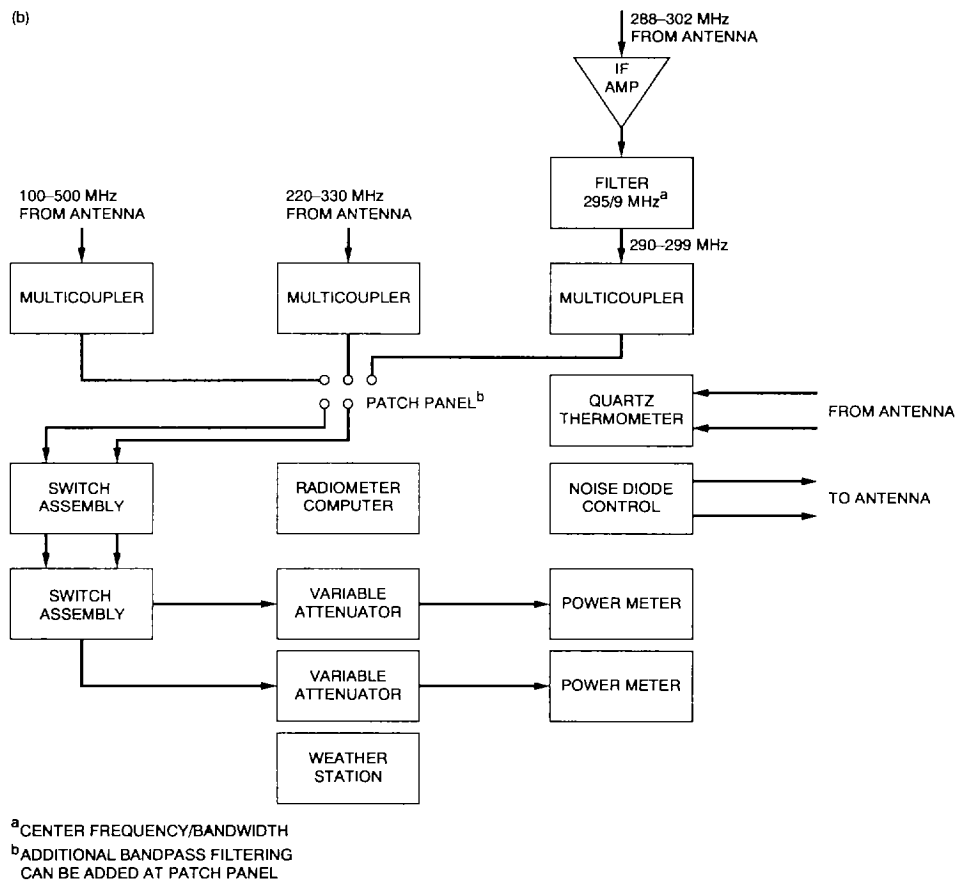


Fig. 1 (contd).

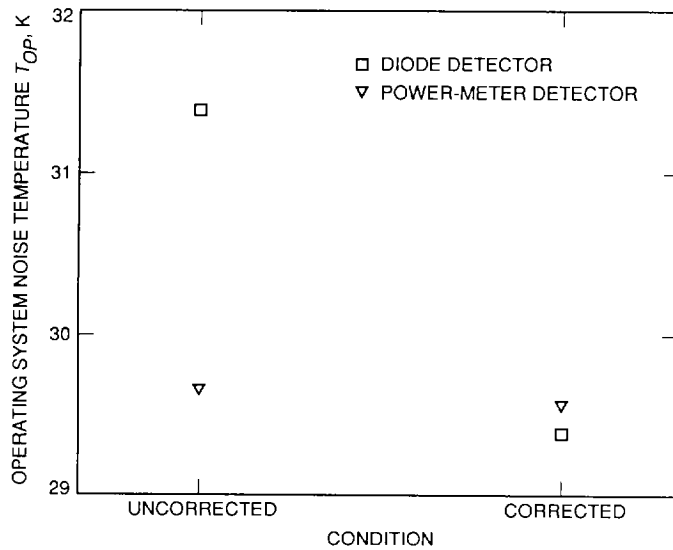


Fig. 2. Comparison of DSS-13 26-m 1988 DOY 271 S-band total power radiometer with power-meter and diode detector configuration noise temperature measurements uncorrected and corrected for nonlinearity.

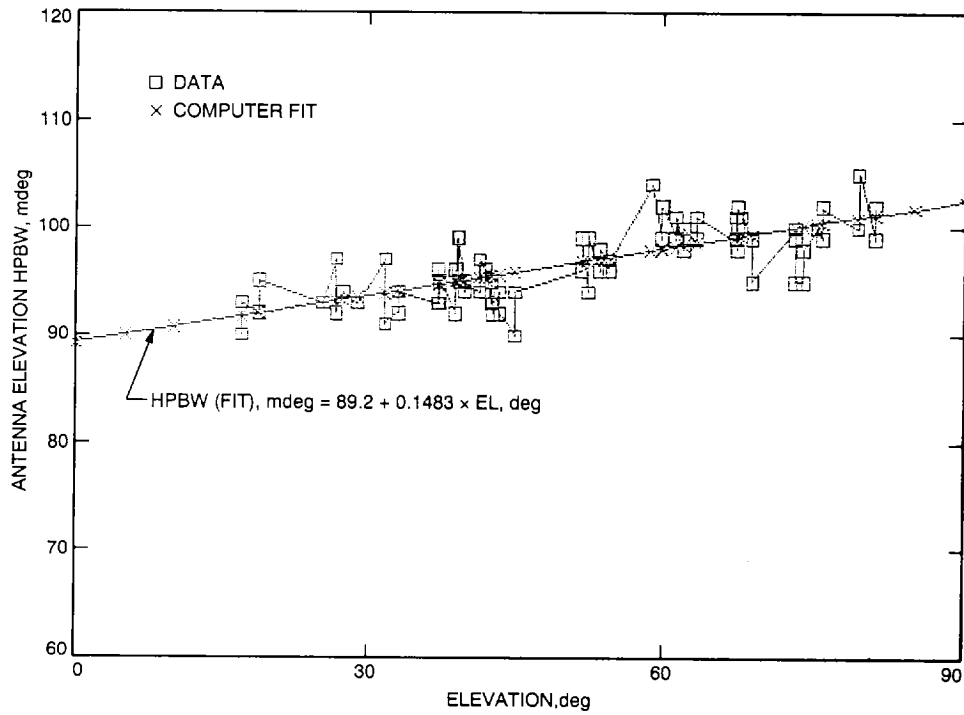


Fig. 3. DSS-13 26-m antenna elevation X-band half-power beamwidth (HPBW) versus elevation angle, December 14, 1989.

DSS13 OBSERVATION LOG

DATE 18 DEC 91 DOY 352 OPERATOR G. Bury PAGE 1 OF 3

SOURCE 1831-21 TYPE SCHEDULE X/S HA/DEC x AZ/EL

CHAN 1 RF FREQ 8437-8451 MHZ IF FREQ 337-351 MHZ (RCP) LCP DET PM

CHAN 2 RF FREQ 2290-2299 MHZ IF FREQ 290-299 MHZ (RCP) LCP DET PM

RF SOURCES OFF? Yes ATTENUATION: IF1 7 dBm /IF2 5 dBm FOCUS 258

FILE#	SOURCE	UT	AZ/EL	DIRECT OFFSETS AZ/EL	UT START TIMES OF SCHEDULED EVENTS	CONK TEMP#1/#2
-------	--------	----	-------	----------------------------	---------------------------------------	-------------------

1X91352	DR21	1624	052 / 20.5	115 / -0.44	1627 1632 1637 1642	18.29 / 18.0
---------	------	------	------------	-------------	---------------------	--------------

BORESIGHT: BLIND? x MANUAL? AUTO? WIND? 4 MPH SKY? PARTLY CLOUDY MINICAL? x PRECAL?

comments: RFI BP 894.6 TC 8.02 RH 77.44

2X91352	DR21	1651	055 / 26.9	116 / -043	1709 1714 1719 1724	18.78 / 18.5
---------	------	------	------------	------------	---------------------	--------------

BORESIGHT: BLIND? x MANUAL? AUTO? WIND? 13 MPH SKY? PARTLY CLOUDY MINICAL? x PRECAL?

comments: RFI

3X91352	DR21	1737	58 / 32	116 / -042	1739 1744 1749 1754	1933 / 18
---------	------	------	---------	------------	---------------------	-----------

BORESIGHT: BLIND? x MANUAL? AUTO? WIND? 10.8 MPH SKY? PARTLY CLOUDY MINICAL? x PRECAL?

comments: RFI

4X91352	1831-21	1803	141 / 23	109 / .053	1804 1809 1814 1819	19.52 / 19
---------	---------	------	----------	------------	---------------------	------------

BORESIGHT: BLIND? x MANUAL? AUTO? WIND? 8.7 MPH SKY? PARTLY CLOUDY MINICAL? x PRECAL?

comments: RFI Edit UT 1819, 1822 Hung up

5X91352	1831-21	1824	146 / 25.9	108 / -052	1828 1833 1838 1843	19.25 / 19
---------	---------	------	------------	------------	---------------------	------------

BORESIGHT: BLIND? x MANUAL? AUTO? WIND? 9.7 MPH SKY? MINICAL? x PRECAL?

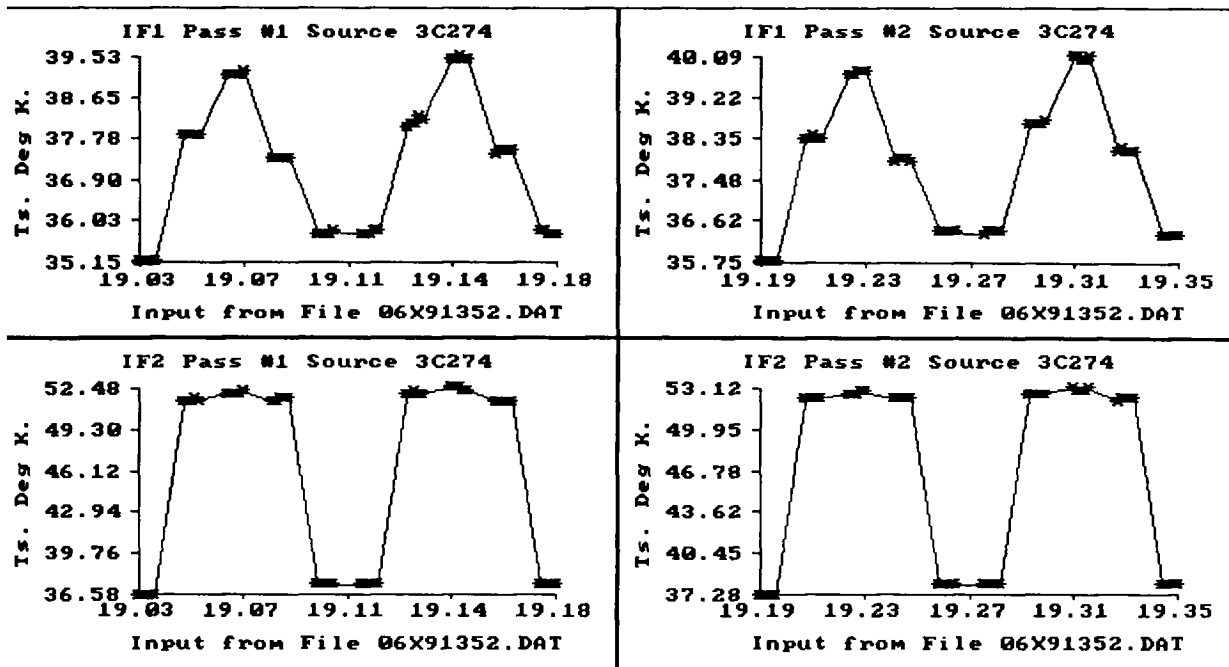
comments: RFI

6X91352	3C274	1902	267 / 24.8	105 / -029	1901 1906 1911 1916	18.99 / 19
---------	-------	------	------------	------------	---------------------	------------

BORESIGHT: BLIND? x MANUAL? AUTO? WIND? 8.9 MPH SKY? PARTLY CLOUDY MINICAL? x PRECAL?

comments: RFI

Fig. 4. DSS-13 26-m antenna observation log for 1991 DOY 352 (transcribed).



Total Power Radiometer Analysis Program Dated 28 January 1992											
Source	3C274	R.A.	12:30:25.7	Dec.	+12:25:57	Fix Az	Off	0.105			
IF1 Rx	NBX	IF2 Rx	NBX	IF2	2294.500	Fix El	Off	0.029			
IF1	8445.000	IF1 BW	12.000	Az.	268.910	IF2 BW		0.000			
Pass 1		MidPass	19.000	Rh.	270.360	El.		0.000			
Pass 2		MidPass	19.110	IF1	82.345	Barom.		894.050			
DOY	352	Temp.(C.)	11.190	File	06X91352.DAT						
		Input	File	Pass	06X91352.DAT						
		IF1Pass1	IF1Pass2	IF2Pass1	IF2Pass2						
I	Az. Corr.	Mean	StDev.	Mean	StDev.	Mean	StDev.	Mean	StDev.		
M	Az. Total	-8.661	0.3658	-7.831	0.4789	-11.658	0.7403	-10.510	0.7773		
N	El. Corr.	96.339		97.169		93.342		94.490			
D	El. Total	2.276	0.1592	2.619	0.2452	-2.499	1.4578	-2.536	0.5753		
M	HPBW Ha.	-26.724		-26.390		-31.499		-28.464			
N	HPBW Dec.	89.927	0.7691	89.645	0.8718	367.878	24.6272	368.846	13.1837		
g	System Top	35.617	0.0139	35.221	0.7084	334.579	17.0784	346.174	18.3827		
	Efficiency	0.420	0.0037	0.419	0.0132	37.122	0.0219	37.836	0.0173		
	Eff. Corr.	0.465		0.463	0.0035	0.561	0.0026	0.560	0.0018		
	Path/Zen. DB	0.108	0.0432	0.118	0.0432	0.079	0.0316	0.086	0.0316		
	Theo/Measure	0.330		0.335		0.253		0.326			
	Perf. Test	2.519		2.335		2.300		1.629			
	IslnCorr.	3.701	0.0325	3.266	0.0310	15.116	0.0695	15.000	0.0496		
	Corr. Pts.	1.024		1.025		1.002		1.000			
	Corr. El.	1.002		1.001		1.001		1.000			
	Corr. Atmos.	1.025		1.025		1.018		1.020			
	Corr. Size	1.054		1.054		1.035		1.035			

Fig. 5. DSS-13 26-m antenna 1991 DOY 352 5-point measurement of radio source calibrator 3C274 used for 1830-211 flux determination.

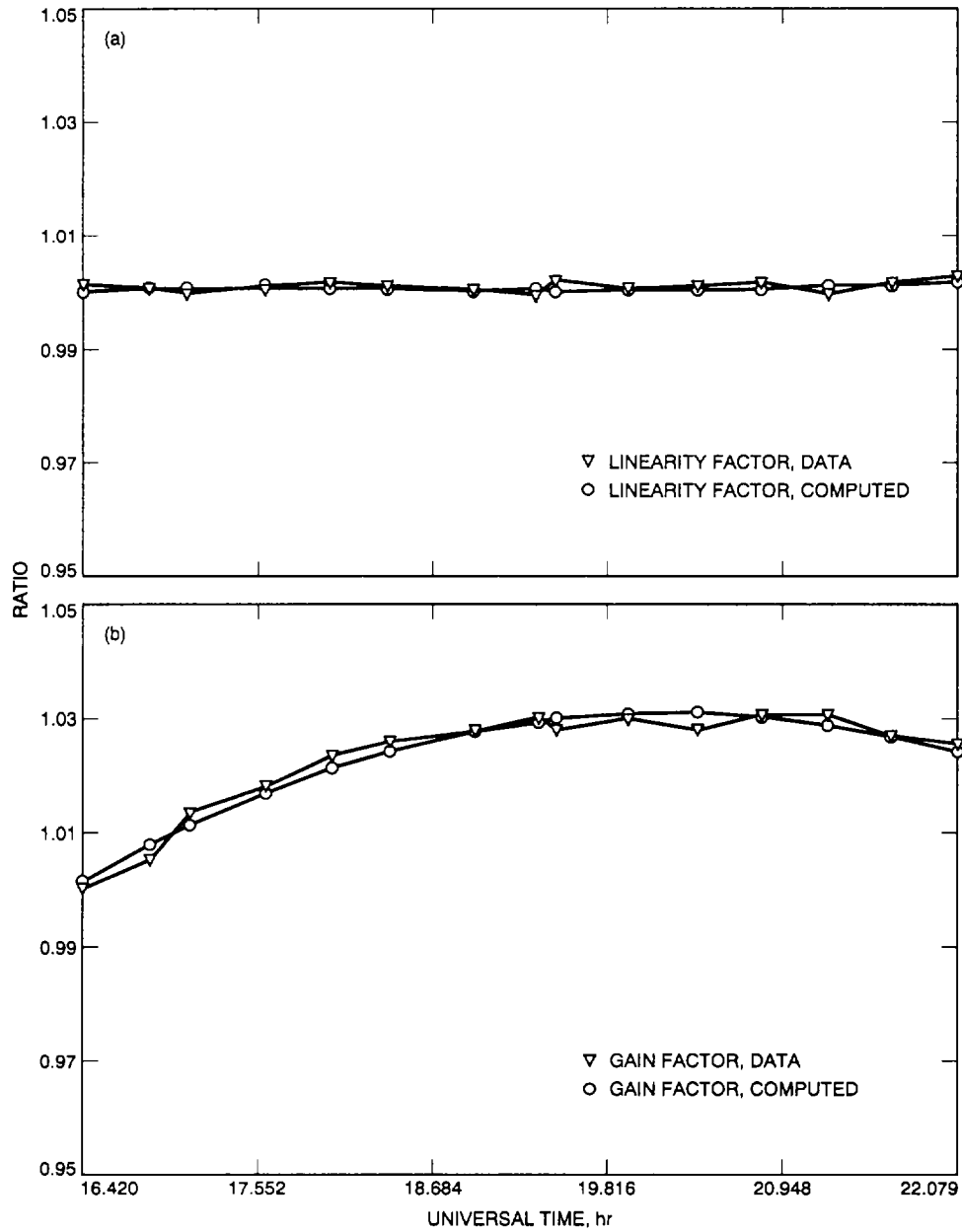


Fig. 6. DSS-13 26-m antenna radiometer X-band calibrations for radio source 1830-211: (a) linearity and (b) gain.

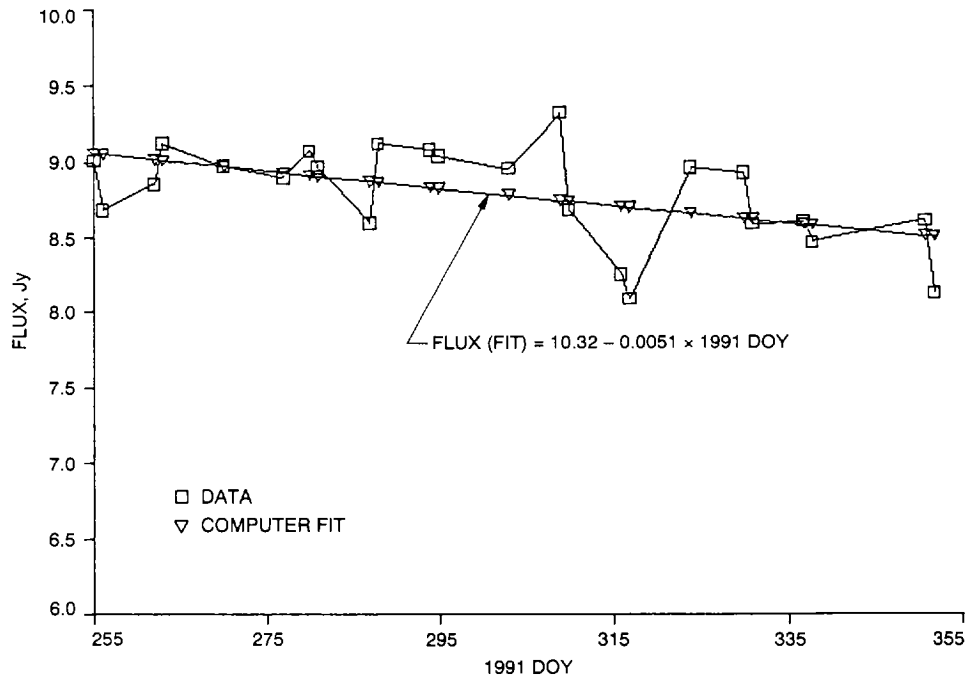


Fig. 8. 1830-211 radio source S-band flux as measured at DSS-13 26-m antenna during 1991.

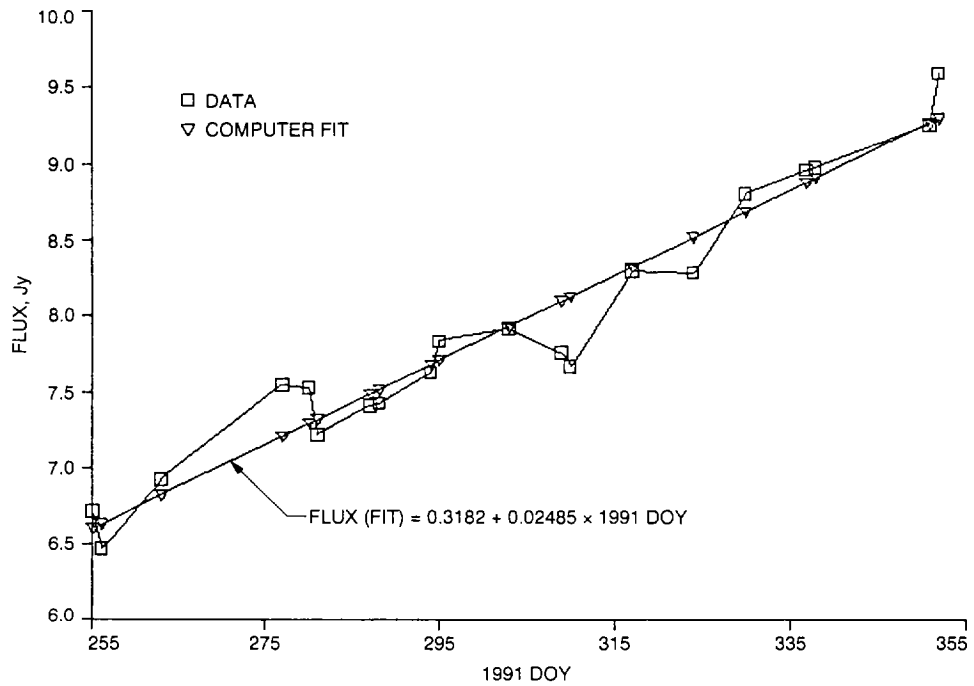


Fig. 9. 1830-211 radio source X-band flux as measured at DSS-13 26-m antenna during 1991.